Heliyon 5 (2019) e01688

Contents lists available at ScienceDirect

Heliyon

journal homepage: www.heliyon.com

Preparation of luliconazole nanocrystals loaded hydrogel for improvement of dissolution and antifungal activity

Manish Kumar [a,b,*], Nithya Shanthi [a], Arun Kumar Mahato [a], Shashank Soni [a], P.S. Rajnikanth [b]

[a] Department of Pharmaceutical Sciences, Sardar Bhagwan Singh Post Graduate Institute of Biomedical Science and Research, Balawala, Dehradun, Uttarakhand, India
[b] Department of Pharmaceutical Sciences, Babasaheb Bhimrao Ambedkar University (A Central University), Lucknow, Uttar Pradesh, India

ARTICLE INFO

Keyword:
Pharmaceutical science

ABSTRACT

Superficial fungal infection in immunocompromised patients can lead to many disorders and complications. Currently, new topical treatment options are critically needed to treat these fungal infections. Luliconazole (LZL) is a topical antifungal medicine used for fungal infection treatment. The purpose of this paper was to develop a new topical luliconazole nanocrystal (LNC) incorporated hydrogel. This study suggested the potential benefits of LNC embedded in a gel as a drug delivery system for topical antifungal treatments. Preliminary experiments were therefore carried out to characterize the LNC in comparison with raw drug. Prepared gel was homogeneous for human use with about 88 percent trapping, non-irritant and safe. Nano-systems showed an overall 5 fold enhancement in solubility, 4 fold increase in dissolution velocity, higher skin retention and better antifungal activity. Drugs retained from LNC hydrogel (N-GEL) in different skin layers within 8 h were the highest, i.e. 62.17% compared to coarse suspension (41.87%), nanosuspension (49.77%), D-GEL (55.76%). In addition, LNC and N-GEL had higher ZOI (41.20 ± 0.61mm and 44.25 ± 0.57mm respectively) than LZL and D-GEL (35.98 ± 0.81mm and 36.83 ± 0.83mm respectively). Therefore, it was observed that LNC loaded hydrogel was more effective in killing the fungus. Consequently, hydrogel incorporated with LNC could be a new approach with improved activity and increased dermal delivery for drugs with poor aqueous solubility rather than coarse drug containing gel.

1. Introduction

LZL is a topical broad-spectrum antifungal drug, approved by the FDA (USA) in November 2013 [1] LZL has lower aqueous solubility that limits dermal bioavailability and acts as a barrier to topical delivery [1, 2]. The solubility of the drug in the lipid phase of stratum corneum also acts as a rate-limiting step for permeation [3]. Fungal infection involves epidermis, dermis as well as deeper layers of skin that require to customize the drug delivery in such a way which localize high drug concentrations at epidermis and dermis layers. However, the commercial topical formulation of LZL (1%w/v cream LUZU®) is associated with lower skin permeation and shorter skin retention of drug [1]. In recent years, the nano-carriers based topical formulation such as nanoparticle, nanoemulsion, lipid nanoparticle, nanocrystals etc. have gained a great importance as a potential drug carrier for topical delivery due to their unique advantages and great versatility as compared to conventional formulations. Presently nanocrystals have gained an increasing interest and found to be superior to other nano-particulate system due to high drug payload capacity, use of minute quantity of excipients, higher chemical stability, lower toxicity, easy scale up and manufacturing [4]. Drug nanocrystals are crystalline nanosized particles with a 100% drug load. Nanocrystals are produced as a liquid dispersion and consist of raw drug stabilized with a polymer or surfactant [5, 6]. Drug preparation as nanocrystals improve bioavailability and skin penetration due to improved solubility and prolonged retention at site of infection [7, 8]. The synergistic effect of the dermal delivery observed with nanocrystals was depot formation in hair follicles and increased penetration. The increased penetration resulting from the nanocrystals will be due to improved saturation solubility. Therefore, resulting in increased concentration gradient between skin and formulation in the initial stage, followed in the later stage by maintaining the concentration gradient between the follicular space and the surrounding cells [9].

In present work, the prepared nanocrystals of LZL was incorporated into hydroalcoholic gel for providing improved drug penetration and skin retention at site of infection. Hydrogels are crosslinked in a three-dimensional arrangement with the advantages of having porosity in the

* Corresponding author.
E-mail address: manishmak333@gmail.com (M. Kumar).

https://doi.org/10.1016/j.heliyon.2019.e01688
Received 24 December 2018; Received in revised form 1 April 2019; Accepted 7 May 2019

gel matrix that allows the loading of hydrophilic or hydrophobic drugs. They have high water content, bioadhesive nature, high biocompatibility, biodegradability and form deposits from which drugs slowly elute into surrounding tissues, maintaining a high local concentration over a long period of time [10, 11]These are good alternatives to oil-based ointment, convenient for topical application with ease [12]. The hydro-alcoholic gel used in this study consists of water and alcohol (PEG, propylene glycol) containing a gel-type mixture. Propylene glycol acts as a cosolvent and penetration enhancer while ethanol acts as a cosolvent to facilitate the distribution of drugs in gel [13]. Ethanol plays an important role in increasing the concentration of low aqueous soluble and hydrophobic drugs in stratum corneum for permeation, resulting in synergistic action [14].

Therefore, the aim of the study was to prepare and characterize LNC loaded hydrogel as potential carrier for topical delivery. Here firstly, LNC were prepared by modified nanoprecipitation method, which were later used for incorporation into the prepared hydrogel base. The optimized LNC loaded hydrogel formulation were evaluated for its particle size distribution, in vitro drug permeation through excised rat skin, in vivo skin retention study in different layers of skin, in vitro antifungal activity and skin irritation study. The results of the study showed that N-Gel showed highest retention of drug into skin and wider zone of inhibition compared to D-Gel.

2. Material and method

2.1. Materials

LZL was obtained as a gift from Virupaksh Organics Ltd., Telangana, India; Vit. E TPGS received as a gift from Antares Health Products Inc., Bhiwandi, India; HPMC K100 and Carbopol 934P acquired from HiMedia Laboratories Pvt. Ltd., India; Candida albicans (MTCC No 183) bought from CSIR-IMT, Chandigarh, India.

2.2. Preformulation studies

2.2.1. Determination of Aqueous Solubility

Saturation shake - flask method was used to determine LZL's aqueous solubility. The excess amount of LZL was dispersed in distilled water and shaken at 50rpm and 37 °C for 72h, filtered and analyzed at a λmax of 299 nm using UV spectroscopy [15, 16].

2.2.2. Determination of lipophilicity

The traditional shake flask method was used to determine lipophilicity. LZL was placed into a flask and measured volumes of n-octanol and aqueous buffer (acetate buffer pH 5.5) were added. The flask was agitated for 72h to achieve equilibrium. The solution was transferred to a separating funnel and left aside for half an hour to separate the two phases. The test compound in each phase was sampled and quantitated using UV spectrophotometer at wavelength of 299nm. The ratio of obtained concentration in n-octanol phase to the concentration in the buffer phase was determined and the $\log_{10}$ P of the ratio was calculated [17].

2.3. Compatibility study

FTIR analysis for LZL, Vit. E TPGS, Physical Mixture (LZL: Vit. E TPGS in 1:1) and LNC was performed by FTIR NICOLET 6700. Each sample was mixed in 1:100 with potassium bromide and later compressed into pellets observed from 4000 to 400cm^{-1}.

2.4. Preparation of LNC

The modified method of nanoprecipitation used in this study was adopted from studies conducted by Bilati, U. et al., 2005; Geng, T. et al., 2017; Choi, J.S. and Park, J.S., 2016; Mishra, B. et al., 2015 with some minor modifications. Vit. E TPGS (0.1–1%w/v) was employed as a dispersion stabilizer. Initially, 10ml organic solution (0.05%w/v of drug in methanol) was added to 50ml of aqueous Vit. E TPGS solution using a 22 gauze syringe while continuously stirring at 2000rpm with a mechanical stirrer (Remi Electrotechnik Limited). The aqueous solution was maintained at 2 °C using ice bath while stirring for immediate precipitation, preventing crystal growth and acquiring a uniform size distribution. Rapid addition of organic phase to aqueous phase maintained at 2 °C resulted in immediate precipitation from antisolvent. Formed dispersion was stirred at 2000rpm for additional half hour and probe sonicated (Sonics Vibro Cell, 20 kHz, 1500 Watt) for 30 min at pulse rate 30/30 while maintaining the dispersion at 25 °C. LNC was collected by centrifuging for 10 min at 4 °C and 10000rpm using a high speed cooling centrifuge (Remi C-24 BL). For modifying the LNC surface, LNC was redispersed in 1% HPMC for an interval of time while stirring to obtain modified nanocrystals, collected by centrifugation at 10000 rpm at 4 °C and then re-dispersed in distilled water, filtered (Whatmann filter paper 0.2μm) and dried at room temperature [18, 19, 20, 21].

2.5. Evaluation of nanocrystals

2.5.1. Particle size and size distribution

Dynamic light scattering was used to determine particle size of nanosuspension in distilled water using Zetasizer Model ZEN3690 Ver. 7.03 Serial Number: MAL1093032 (Malvern Instruments, UK). Average particle size diameter (ZAve) and polydispersity index (PDI) reflecting mean particle diameter and size distribution width were measured parameters.

2.5.2. Determination of drug content

Drug content of prepared LNC dried at room temperature was determined using UV-visible Spectrophotometer (Shimadzu 1800). 5mg of nanocrystals was dissolved in 10ml methanol in a 10ml volumetric flask followed by filtration (Whatmann filter paper 0.2μm). Concentration of filtrate was determined spectrophotometrically at a λmax of 299nm [15].

2.5.3. Determination of solubility

LNC in excess was dispersed in distilled water and acetate buffer pH 5.5 and subjected to the shaking at 50rpm and 37 °C for 72h to attain equilibrium, filtered (Whatmann filter paper 0.2μm) and analyzed at 299nm using UV-Visible spectrophotometer [16].

2.5.4. In-vitro dissolution study

The in vitro powder dissolution study of LZL and LNC was determined using USP Apparatus 2 dissolution tester [22]. The dissolution test was carried out in 900ml of pH 5.5 acetate buffer with rotating speed of 50rpm and temperature maintained at 37 ± 0.5 °C. An equivalent amount of drug was introduced directly into the dissolution medium. At predetermined time interval, 5ml of sample was withdrawn and replaced with fresh medium. Samples were filtered (Whatmann filter paper 0.2μm) and analyzed at observed λmax 299nm (Model: UV-1800 Shimadzu). Three replicate dissolution tests were performed for each formulation [16, 23].

2.5.5. Short term stability study

Effect of temperature: For stability testing of prepared nanosuspension, selected samples were stored at room temperature, 2 °C and 40 °C. The particle size was analyzed on 0, 1 and 7 days of storage [24, 25].

Effect of thermocycling: Nanosuspension was stored at 2 °C for 24h followed by storage at 40 °C for next 24h for one cycle. After four cycles, particle size and zeta potential were determined [24].

2.5.6. Scanning electron microscopy (SEM)

The morphology of LZL and LNC was examined by SEM (LEO, model no. 435 VP, England). A small quantity of drug nanocrystals was placed

on the surface of metal stubs by aid of adhesive tape and was gold coated with a sputter coater for preparation of sample.

2.5.7. Powder X-Ray diffraction (PXRD)

PXRD analysis was performed for LZL, physical mixture (LZL: Vit. E TPGS in 1:1) and LNC using D8 Advanced Diffractometer (Bruker AXS D8 Advance, Serial Nr- D8-03/202035 D76181 Karlsruhe, Germany at scanning rate of 2 °C/min over a 2θ range of 5–40 °C.

2.5.8. Differential scanning calorimetry (DSC)

DSC was performed using instrument EXSTAR TG/DTA 6300. In DSC analysis 10 mg of sample was placed in an aluminium pan and examined at scanning rate of 10 °C/min at temperature range of 0–800 °C in an inert atmosphere maintained with nitrogen.

2.6. Preparation of gel

Firstly gel base was prepared by dispersing the Carbopol 934P into known quantity of water while continuously stirring at 600rpm followed by addition of methyl paraben sodium (0.02%w/v) and propyl paraben sodium (0.1%w/v) and was stirred for additional half hour. Prepared gel base was kept aside for a period of 24h. Secondly LZL (0.5%w/w) and LNC (0.5%w/w) was dispersed in appropriate quantity of propylene glycol (5%w/w) and 1% ethanol (20%w/w) later added to carbopol gel bases while stirring at 1000rpm followed by further agitation for 30min to obtain D-GEL and N-GEL respectively. Tri-ethanol amine (TEA) was added to maintain pH of 5.5–6.5 for maximum efficiency and stirred thoroughly to get clear homogeneous gel [26].

2.7. Evaluation of gel

2.7.1. Determination of pH

Determination of gels' pH was done with the help of Digital pH meter (Systronics). The glass electrode of pH meter was dipped in prepared gel and rotated to measure the pH of gel.

2.7.2. Determination of viscosity

Viscosity of gel was determined with the help of Brookfield Viscometer. The Viscosity of different batches of gel was measured at 50 and 100rpm and compared to select desired viscosity range.

2.7.3. Drug content uniformity

Drug content uniformity study for gel was done to measure the homogeneity of system. In order to measure homogeneity of system, the top, middle, and bottom layers of gel (1g) was taken out and dissolved in methanol. The gel was vortexed (5min) and centrifuged (10min) to extract drug from matrix and the drug content was determined using UV Visible Spectrophotometer.

2.7.4. Skin irritation study

Skin irritation study of gel was assessed on male albino Wistar rats 110–125g after receiving an approval from Control and Supervision of Experiments on Animals, CPCSEA Committee (**CPCSEA/IAEC/SBS/2017–18/0015**). The formulation was applied on 1cm^2 region of skin and left exposed for 48h. The application site was wiped with water and examined for the dermal reaction (edema and erythema) after predetermined interval [27, 28]. Area was inspected visually according to irritation score method reported by Dreher F. et al. 1996 for judging erythema graded as 0 no erythema, 1 slight redness (spotty or diffused), 2 moderate uniform redness, 3 intense redness, 4 fiery red with edema [28].

2.8. Ex-Vivo drug permeation studies

Male albino Wistar rats of 5–6 weeks old weighing 110–125g were used. Informed consent has been obtained for experimentation with animal subjects (CPCSEA/IAEC/SBS/2017–18/0015). Rats were sacrificed, shaved and excised from the dorsal region of skin. Skin was mounted on Franz diffusion vertical cells between receptor compartment and donor compartment facing the stratum corneum (SC). The receptor was filled with 7.5ml physiological saline solution (pH 7.4 buffer: methanol as 9:1 to provide sink condition) continuously stirred at 50rpm and thermostated at 37 ± 0.5 °C. Coarse Suspension and Drug Nanosuspension (5mg each ml), D-GEL and N-GEL (5mg each gram) was applied to the skin surface and complete emptying of the receiving solution was made at predetermined time intervals with replacement with the fresh solution after each sampling. Finally aliquots were filtered and analyzed at 299nm for drug content. After 8h, the skin specimens was gently washed, Subcutaneous (SC) and Epidermis (EP) were separated from the dermis (DE) with a scalpel. SC, EP and DE were cut and placed in a flask with methanol to sonicate for 10 min for extracting the drug. Tissue suspensions were centrifuged at 3000rpm for 10 min, filtered and assayed for drug content. Cumulative amount of drug was plotted as a function of time [27, 29].

2.9. Antifungal study

Using Candida albicans (MTCC No 183), an in vitro inhibition zone assay was conducted. Filling 25mL of Sabgroud Dextrose Agar into a petri dish prepared the agar plates. Two wells with volumes of 100μL were punched into the agar plate after solidification. To avoid the growth of other undesirable microorganisms except for Candida albicans, all plates were sterilized at 121 °C for 15min before use, followed by a uniform spread of 100μL Candida albicans (4 × 106 cfu/ml) across the entire agar surface using a sterilized spreader rod. After 1 h of rest, 100μL of LZL suspension (1 mg/ml) as control and 100μL of LNC nanosuspension (LNC equivalent to 1 mg LZL/1ml) as test were filled into two separate wells in a plate and 100mg each of D-Gel and N-GEL into two separate wells of other plate were filled. All plates were incubated for 72 h at 30 °C. The inhibition zone assay samples were examined in triplicate [30].

2.10. Statistical analysis

All results were statistically analyzed using version 6.05 of graph pad prism. The results were shown with standard deviation (SD) in mean (*n = 3). For group comparison, ANOVA and Student's t - test were used. The statistical significance at p 0.05 has been set.

3. Results

3.1. Preformulation studies

Preformulation studies have been conducted to determine the physicochemical properties of the drug (e.g. solubility and permeability). LZL compatibility with excipients has been determined to prevent the problem of incompatibility. LZL solubility has been obtained as 0.003435 ± 0.00678 mg/ml and 0.003356 ± 0.000102 mg/ml in aqueous and acetate buffer (pH 5.5) reflecting poor solubility. In addition, the non-aqueous solubility was found to be 18.734 ± 0.24 mg/ml for LZL in n-octanol. The LZL's lipophilicity was successfully determined where $\log_{10}$ P was obtained as 3.75 near the reported value of 4.07 [1]. Luliconazole has therefore been concluded to be a drug of BCS Class II.

FTIR analysis for LZL, Vitamin E TPGS, physical mixture and LNC was successfully conducted (Fig. 1). The FTIR analysis of LZL showed absorption at 3039.39, 3076 & 3119cm-1 for Aromatic C–H Stretching, 2941 for C–H aliphatic stretching, 2527 & 2614cm-1 for S–H Stretching, 2199.08 for C≡N Stretching, 1698cm-1, 1737, 1816, 1892 for C=C Alkene Stretching, 1634cm-1 for C=N Stretching, 1555.96cm-1 for C=C Aromatic Stretching and 761 & 1100cm-1 for C–Cl Stretching. Spectra of Vit E TPGS showed absorption at 2916.5 for C–H aliphatic stretching, 1465, 1574.6, 1643 C=C for aromatic stretching, 742.7 for C–Cl stretch and 3474 for O–H stretching. Physical mixture showed band at 3039,

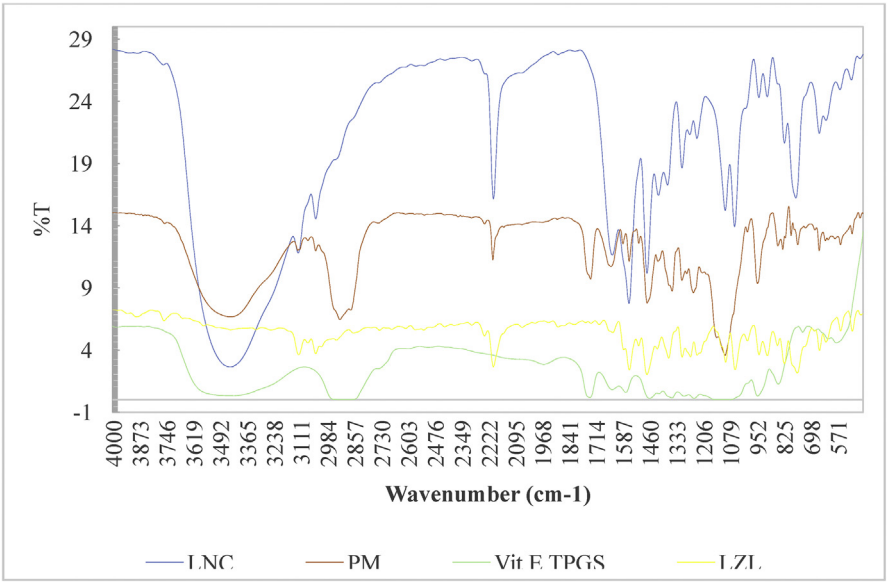

Fig. 1. FTIR Spectra for luliconazole (LZL), Vitamin E TPGS, Physical Mixture of drug and Vitamin E TPGS in 1:1 (PM) and luliconazole nanocrystals (LNC F 19).

3124 for C–H Aromatic stretching, 2925 C–H aliphatic stretching, 2201, 2240 C≡N Stretching, 1642 C=N- stretching, 1471, 1557 C=C aromatic stretching, 1471, 1586 Aromatic C=C for Chlorobenzene, 759 C–Cl stretch and 3440 for O–H stretching. No difference was observed in the absorption band for chemical bonding of pure drug and vitamin E TPGS. This revealed the compatibility of luliconazole with vitamin E TPGS. Furthermore, bands for LNC found that there were not many peaks observed with LZL alone (2941 C–H aliphatic stretch, 2527, 2614 S–H Stretching, 1698, 1737, 1816, 1892 C= C Alkene Stretching) although peaks for vitamin E TPGS (3441 O–H Stretch, 3) were observed. This reflected proper LZL encapsulation within the stabilizer protective layer.

3.2. Development of method

Modified nanoprecipitation method has been selected as an ideal method for the preparation of luliconazole nanocrystals involving temperature maintenance at both treatment phases, i.e. nanoprecipitation and cooling sonication probe. Step by step Optimization was performed for stirrer speed, solvent system, stabilizer concentration, and temperature to bring microcrystals in nano-range. For the preparation of luliconazole nanocrystals, methanol as solvent, 2000rpm velocity, concentration ranging from 0.1 to 1% w/v and temperature control of 2 °C in the first phase and 25 °C in the second phase were selected (Table 1). The rapid addition of organic phase to aqueous phase maintained at 2 °C in modified method resulted in immediate precipitation from antisolvent also reported by Geng, T et al., 2017 [19]. Temperature control at the initial stage of nanoprecipitation helped to achieve homogeneity as a result of which smaller nanocrystals with lower PDI were obtained on cool probe sonication. The combination resulted in similar results to combinations such as bead milling with HPH which increased homogeneity by decreasing larger crystals and aggregates of bead milling [9, 25].

3.3. Evaluation of nanocrystals

3.3.1. Determination of particle size

Nanocrystals were successfully prepared where the size and PDI value of Vit. E TPGS increased from 0.263 to 0.896μm and 0.093 to 0.96 respectively (Table 2). Results were obtained in contrast to Ghosh I et al., 2011, where size decreased with increasing Vit. E TPGS concentration [31]. The size of prepared nanocrystals was between 0.263-0.611μm, close to the reported value of 0.25 and 0.66 μm, which are optimal for fast dissolution and hair depot formation, respectively, as Zhai X et al. concluded in 2014 [25]. Particles from 0.2 to 0.6μm may penetrate deeply and locate in hair follicles [9].

3.3.2. Determination of drug content, % entrapment and solubility

Drug content, percentage of trapping and solubility have been successfully determined. Each LNC 5 mg found 4.66 mg LZL with 93.206 percent w/w entrapment. Similar drug trapping (90–95% w/w) was also reported for Ige P. P. et al. 2013 nanosuspension [6]. LNC water solubility was found to be 0.015809 ± 0.001752 mg/ml, i.e. 5 times the LZL

Table 1
Optimization table for speed, solvent and concentration.

Formulation code	Concentration of Vit. E TPGS (%w/v)	Speed (rpm)	Solvent	Size (μm)	PDI
F1	0.25	1000	Ethanol	15.3	0.238
F2	0.25	**2000**	Ethanol	2.795	0.350
F3	0.25	4000	Ethanol	4.996	0.815
F4	0.25	6000	Ethanol	18.6	1
F5	0.25	2000	Propanol	3.689	0.656
F6	**0.25**	2000	**Methanol**	2.272	0.287
F7	**0.1**	2000	Methanol	2.312	0.312
F8	**0.5**	2000	Methanol	2.648	0.572
F9	**0.75**	2000	Methanol	3.747	0.717
F10	**1**	2000	Methanol	4.064	0.853
F11	2	2000	Methanol	5.727	1

Table 2
Effect of temperature control on nanocrystal size.

Concentration of Vit. E TPGS (%w/v)	Formulation code	Method	Size (μm)	PDI
0.25	F12	Nanoprecipitation + Simple Probe Sonication (No temperature control)	28.96	1
	F15	Nanoprecipitation + Cooling Probe Sonication for 15min (temperature controlled)	0.910	1
0.5	F13	Nanoprecipitation + Simple Probe Sonication (No temperature control)	16.5	1
	F16	Nanoprecipitation + Cooling Probe Sonication for 15min (temperature controlled)	0.991	0.731
0.75	F14	Nanoprecipitation + Simple Probe Sonication (No temperature control)	19.3	1
	F17	Nanoprecipitation + Cooling Probe Sonication for 15min (temperature controlled)	1.225	0.849
0.05	F 18	Modified Nanoprecipitation method.	0.112	0.353
0.1	F 19		**0.263**	**0.093**
0.25	F 20		0.278	0.254
0.5	F 21		0.506	0.556
0.75	F 22		0.611	0.772

solubility.

3.3.3. Determination of dissolution velocity

LNC and LZL dissolution testing was conducted to determine the effect of nanosizing on the velocity of dissolution. There was a noticeable increase in dissolution and was significantly different ($P < 0.05$). About 7.27 ± 2.41 percent and 27.65 ± 3.63 percent of LZL and LNC respectively were dissolved within 6h (Fig. 3 C).

3.3.4. Stability studies

Effect of Drying: Nanosuspension based on 0.25% w/v vitamin E TPGS analyzed on 0 and 1 day prior to drying showed a slight increase in crystal size. Significant increase in nanocrystals size was observed after drying at room temperature with more pronounced increase in oven drying at 40 °C (Table 3). In addition, a slight decrease in PDI with an increase in nanocrystals size was observed. Results favored the study of Vidlarova L et al., 2016 where it was reported that increased size decreased PDI for nanoparticles based on Plantacare 1200 and 2000 [9].

Effect of Additional Stabilizer: Nanosuspension based on 0.1 percent w/v Vit. E TPGS showed an increase in particle size at room temperature. Particulate size was steady at 2 °C for lower storage temperature. Crystal exposure to higher temperatures, i.e. 40 °C, and drying at room temperature resulted in an increase in particle size. Whereas a slight increase in size was observed with combination nanosuspension based on vitamin E TPGS (0.1 percent w/v) and HPMC (1 percent w/v) stored for a week at room temperature and 40 °C. Nanosuspension stored at different temperatures (thermocycling) was more likely to grow in particle size. In addition, although the combination-based nanocrystal thermocycling process resulted in a larger size, the observed size was still within the nano-range with very low PDI. Thus, the stabilizer combination found to have a synergistic effect on stabilization (Table 4), identical to the observation made by Ghosh I et al. 2012 that prevented agglomeration and crystal growth during processing or its shelf life by providing better steric hindrance [32].

3.3.5. Scanning electron microscopy

LZL and LNC morphology has been successfully identified. LZL with broad size distribution was found to be irregular (Fig. 2 A). LNC was a narrow size plate shaped (Figs. 2B & 2C), similar to the nanosuspension based on TPGS as reported by Yue P. F. et al., 2013 [33].

Table 3
Effect of Drying on Particle size and PDI.

Sample	Storage Condition	Size (μm)	PDI
0.25%w/v Vitamin E TPGS	Room Temp/0 day	0.278	0.254
	Room Temp/1 day	0.289	0.253
	Room Temp/1 week	0.292	0.32
	Dried at Room Temp	0.493	0.112
	Oven Dried (40 °C)	1.438	0.316

3.3.6. X-Ray Powder Diffraction

X Ray Powder Diffraction studies were conducted to determine the stabilizer's influence on the existing LZL state and analyze potential changes in crystalline state after drug formulation as nanocrystals (Fig. 3A). Coarse luliconazole (LZL) showed characteristics peak at $2\theta =$ 15.6857, 17.5783, 20.665, 21.1058, 22.6466, 23.8135, 25.0052, 26.2619, 27.2455, 29.1017and 42.6894 indicating presence of crystalline nature. Diffraction patterns for 1:1 physical mixture of drug and stabilizer were observed at $2\theta =$ 15.8295, 18.8069, 20.8869, 21.3359, 22.96, 24.2447, 25.1518, 27.5892, 30.9059, 33.6395, 34.9483, 35.4005, 39.5721, 41.6825, 42.9524, 44.8374 and 53.8326 with identical peaks for coarse drug. The patterns for Vit. E TPGS stabilized nanocrystals exhibited sharp peaks at $2\theta =$ 21.0533, 22.4937, 24.9074, 26.1712, 30.601, 34.3614, 36.6835, 37.8667, 42.4697, 43.4029, 45.9582, 46.6987, 47.6778, 48.6929, 49.9848 and 51.1346. Diffraction peak observed at $2\theta = 23$ in PXRD pattern represented (021) plane due to two chlorine and a nitrogen atom belonging to cyano group [34]. Patterns observed for LZL and physical mixture were found to be quite similar, probably due to the non-homogenous distribution of the drug to the stabilizer's interior and surface. In addition, the peak at $2\theta = 23$ with LNC was most likely not observed due to the presence of stealth layer around drug stabilizers and thus reflected complete encapsulation of drug within the polymer matrix. Ige P.P. et al., 2013; Kumar R. and Siril P.F., 2017 has achieved similar results [6, 35].

3.3.7. Differential scanning calorimetry (DSC)

The DSC curve for LZL showed a sharp endothermic peak at 149 °C similar to the reported value [42] and a degradation curve at 589 °C, while the LNC showed an endothermic peak at 590 °C (Fig. 3B) with endothermic peak at 151 °C. Thus DSC Curve for LNC revealed the crystalline state to be preserved.

3.4. Optimization of gel

Viscosity and percentage entrapment were assessed for the prepared gel. For the study, 0.75% w/w and 1% w/w carbopol had insufficient viscosity, i.e. 30 and 48cP respectively. 1.5 percent w/w viscosity was sufficiently good (377cP) similar to the gel viscosity reported by Jana S. et al. 2014 [36]. Prepared gel (1.25–2% w/v) was checked for trap efficiency where only 1.25% w/w and 1.5% w/w showed acceptable results (68.8% and 74.4% respectively). Based on reflected viscosity and better trapping, 1.5 percent w/w carbopol gel base was selected as ideal for LNC gel preparation Plastic homogenizer was used as a stirrer to ensure proper mixing, resulting in a homogeneous gel with 88 percent entrapment. Loss in trapping may be due to material adhesion to container surfaces.

3.5. Evaluation of gel

PH, viscosity, spreadability, and trapping were evaluated for the prepared gel. The D-GEL (375 cP) and N-GEL (372.9 cP) viscosity

Table 4
Stability Study for 0.1%w/v Vitamin E TPGS and Combination (0.1%w/v Vitamin E TPGS with 1%w/v HPMC) based Nanocrystals.

Storage Condition/No of Week Exposed		0.1%w/v Vitamin E TPGS		
		Size (μm)*	PDI*	Zeta*
Room Temp/0 day	Sample	**0.263 ± 22.12**	0.093 ± 0.11	-18.36 ± 0.21
Room Temp/1 day		0.312 ± 50.08	0.120 ± 0.10	-18.36 ± 0.23
Room Temp/1 week		**0.446 ± 40.01**	0.94 ± 0.102	-17.6 ± 0.87
2°C/1 week		0.358 ± 51.14	0.15 ± 0.13	-17.36 ± 0.40
40°C/1 week		2.571 ± 405.89	0.80 ± 0.34	-1.81 ± 0.08
Air dried/1 week		2.038 ± 1115.66	0.53 ± 0.40	-1.81 ± 0.14
Room Temp/0 day	+1%w/v HPMC	**0.296 ± 11**	0.53 ± 0.19	-19.1 ± 0.21
Room Temp/1 day		0.335 ± 39.43	0.502 ± 0.49	-19.1 ± 0.23
Room Temp/1 week		**0.352 ± 50.57**	0.12 ± 0.072	-19.07 ± 0.66
2°C/1 week		0.405 ± 50.20	0.76 ± 0.25	-19.07 ± 0.66
40°C/1 week		0.562 ± 33.24	0.26 ± 0.16	-19.5 ± 0.30
Air dried/1 week		0.833 ± 252.54	0.44 ± 0.49	-19.0 ± 0.26
40 °C for 1 h and 2 °C for 1h 3 cycle/1 week (thermos-cycling)		0.664 ± 49.51	0.12 ± 0.041	-18.60

*$n=3$, mean ± SD.

observed were equivalent to the desired value and suitable for use. Gel pH was about 5.8 ± 0.06 close to the pH of normal human skin and had good spreadability of the skin surface. Percentage entrapment was found to be 88 percent with homogeneity throughout the different layers of gel for both formulation with developed method.

3.5.1. Skin irritation study

In order to confirm the safety of formulated gel, skin irritation test was conducted. Even after 48h, the formulation did not show any erythemal and edemal scores. The average skin irritation score was 0.33 (slight redness in a rat) which is less than 5 indicating the non-irritating nature of gel when applied to human skin [28]. All excipients used in the formulation were therefore found to be non-irritating and safe for topical application.

3.6. Ex-Vivo permeation study

Using Franz diffusion cell, Ex-Vivo permeation study from coarse suspension, nanosuspension, D-GEL and N-GEL was successfully carried out on rat skin. No significant difference was observed in drug permeation rate across the skin due to coarse suspension and nanosuspension or D-GEL and N-GEL ($P < 0.05$). The drug permeated with coarse suspension, nanosuspension, D-GEL and N-GEL was approximately 128, 163, 93 and 77μg respectively within 2h and 154.78, 200.15, 154.32 and 119.65μg respectively within 6h.

Cumulative skin-permeated drug from N-GEL (4.79 %) compared to D-GEL (6.18 %) was found to be significantly different within 6 h ($P < 0.05$), whereas no significant difference was observed for nanosuspension and coarse suspension. Thus, N-GEL retained a larger amount of drug into the skin layer. The percentage of drugs retained within 8 h from coarse suspension, nanosuspension, D-GEL and N-GEL was approximately 41.87, 49.77, 55.76 and 62.17 respectively (Fig. 4B) where the retention rate with nanosized systems was higher.

3.7. In-vitro antifungal activity study

In vitro antifungal activity for LZL, LNC, D-GEL and N-GEL has been performed. To determine antifungal activity, the mean inhibition zone (ZOI) for Candida albicans was calculated. Compared to LZL with a ZOI diameter of 35.98 ± 0.8172 mm, LNC (ZOI 41.20 ± 0.6110 mm) was observed to be more effective in killing fungus. N-GEL also exhibited higher ZOI of 44.25 ± 0.57mm compared to D-GEL (36.83 ± 0.83mm). Microscopy of Candida albicans survived outside the inhibition zone was found to be similar to previously reported, confirming the presence of only Candida albicans [37].

4. Discussion

4.1. Effect of speed in nanosization

The system was continually stirred at varying speeds of 1000–6000rpm. It was seen from Table 1, that 2000rpm resulted in smallest size nanosuspension. Lower speed than 2000rpm resulted in larger particles which may result from insufficient organic phase dispersion [38]. Particulate size increased with mechanical stirrer speed as 2000 (2.795μm) > 4000 (4.996μm) > 6000 (18.6μm) which can be explained by aggregation of particle. Probably higher rpm generated greater force on individual particles as additional mechanical energy which broke the repulsive forces between particles as Ghosh I. et al., 2012 explained and resulted in aggregation of particle [32]. Similar results were observed by Kumar S. et al., 2015 [39].

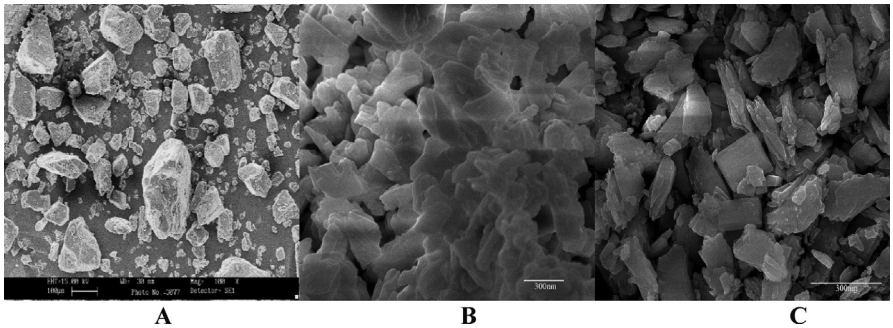

Fig. 2. SEM images for A) luliconazole, B) Vitamin E TPGS based nanocrystals and C) Vitamin E TPGS & 1% HPMC Combination based nanocrystals.

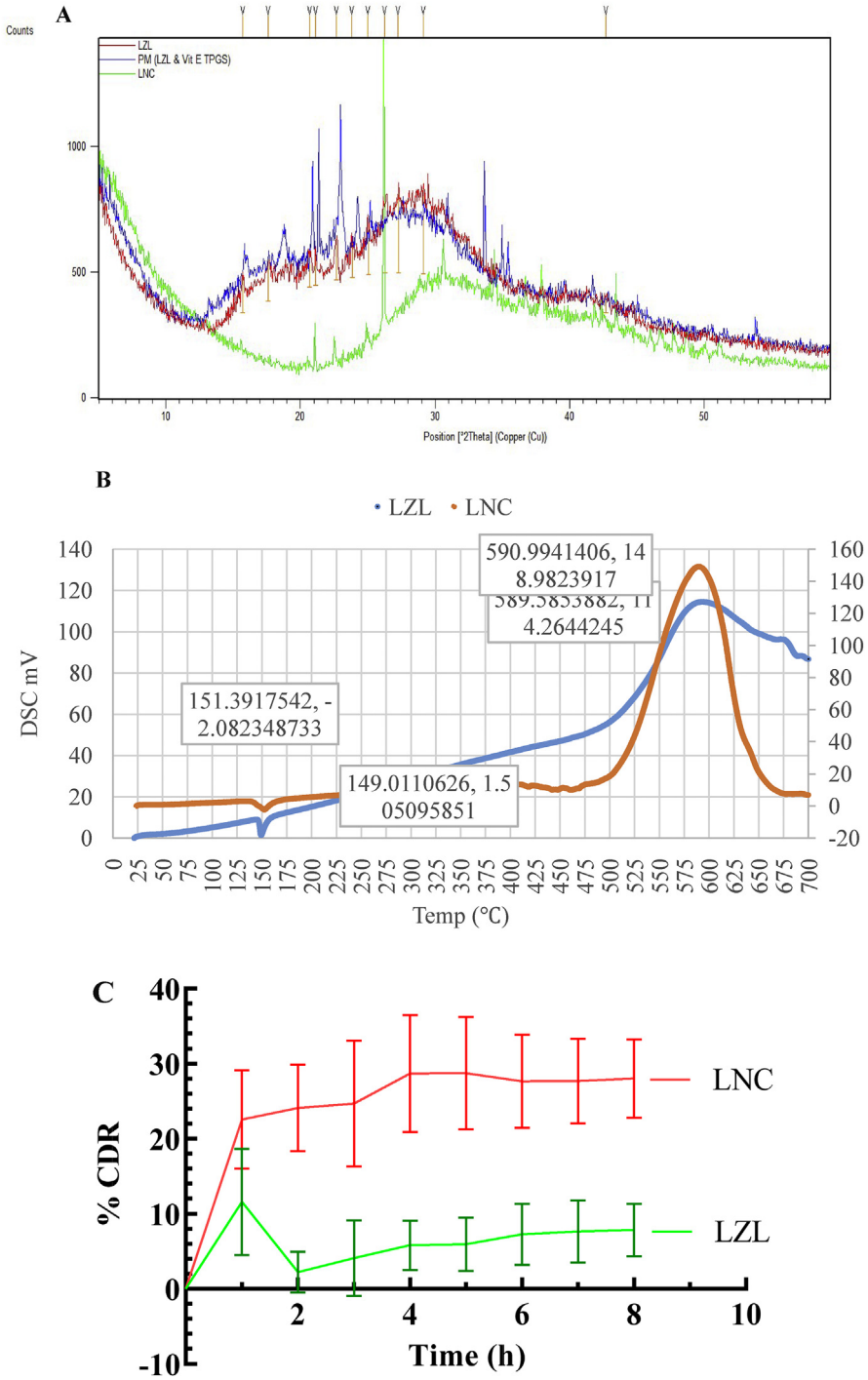

Fig. 3. A. X-Ray Diffraction Pattern for luliconazole (LZL), Physical Mixture of LZL and Vit. E TPGS (1:1) and luliconazole nanocrystals (LNC F 19). B. DSC Curve for luliconazole (LZL) and its nanocrystals (LNC F 19). C. Dissolution Study for luliconazole (LZL) and its nanocrystals (LNC F 19).

4.2. Effect of solvent system in nanosization

Solvent system used for preparation of organic phase was observed to influence the particle size. Methanol produced smaller size particles than ethanol and propanol. Mean size increased in sequence as methanol (2.272μm) > ethanol (2.795μm) > propanol (3.689μm) (Table 1). Possibly methanol may have been higher in diffusion rate of solvent into non-solvent. The rapid diffusion of methanol into the dispersion medium resulted in nanocrystals being formed. Results were identical to the observation concluded by Bilati U. et al., 2005 [18].

4.3. Effect of stabilizer concentration

As demonstrated by Table 2, increased particle size was observed from 0.112 to 0.893μm with increasing concentration of Vit. E TPGS. The result was in contrast to Makhlof A. et al., 2008 study where size decreased with increasing concentration of stabilizer [40]. Particle aggregation or the ripening of Ostwalds could be a possible cause for the increase in particle size. The interactions between the hydrophilic chains of one particle and the hydrophilic chains of another particle, leading to an agglomeration at higher concentrations, might result in particulate aggregation [38]. Particle growth with stabilizer overdosing could also

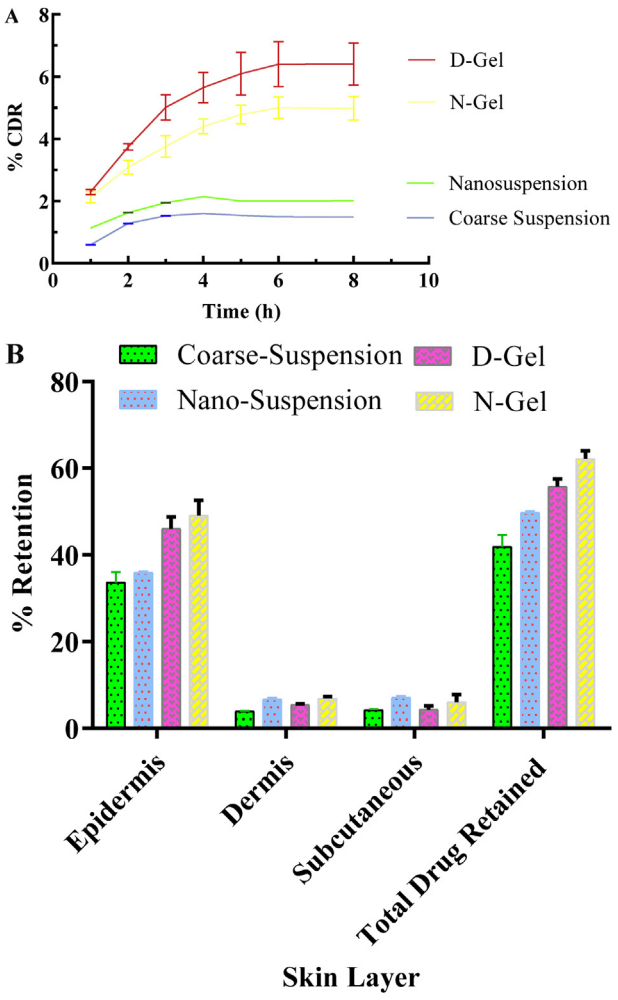

Fig. 4. A. Cumulative amount of Drug Permeated. * D-Gel is gel containing luliconazole, N-Gel is gel containing nanocrystals. B. Drug Retention Profile. * D-Gel is LZL Incorporated Gel, N-Gel is LNC Incorporated Gel.

be due to Ostwalds ripening as stated by Malamatari M. et al., 2018 [4]. Result achieved is in accordance with Colombo M. et al., 2017 where nanocrystals size rose from 0.188 to 0.206μm with increased concentration of Vit. E TPGS from 0.02 to 2%w/v [41].

4.4. Effect of temperature

Table 2 illustrates the effect of the temperature of the dispersion systems on particle size during sonicator therapy. The size increased with simple sonomination as opposed to simple nanoprecipitation due to the heat generation during sonication (Table 2). The sonification of the cooling sond (at 25 °C) led to nanosizing crystals and thus reduced the size of larger, simple nanoprecipitation, crystals. More rapid stabilization has also been observed as a coolant which encourages crystal formation while reducing the dissolution of the crystal by prevention of crystal growth [6, 9, 21]. Likewise Liu D. et al., 2015 prepared nanoparticles by ultrasonicating micro dispersion for 15 min at 4–8 °C and Mishra B. et al., 2015 restricted the Ostwald ripening by keeping antisolvent system at 3 °C while precipitation [21, 42]. Temperature control in both treatment phase i.e. nanoprecipitation and probe sonication showed that size decrease was further reduced due to the weakened recrystallization mechanism which resulted in a homogeneous nanosuspension with lower PDI (Table 2).

4.5. Stability studies

As noted in Table 3, the evident growth of particles after drying could be due to capillary forces encountered [6, 24, 43]. Changed temperature results in the destabilization of adsorbed stabilizers on crystals due to temperature stress [24]. Nanosuspension stored at varying temperatures (thermal cycling) was prone to crystal growth to a greater extent due to a higher rate of solubility change [24]. Coalescence of nanoparticles could be prevented by freezing the sample where a redispersent or cryoprotectant such as maltose or mannitol was added before drying [6, 24, 42]. Theoretically, crystal growth during storage may be due to particle agglomeration or ripening of Ostwalds or both. This observation justified adding HPMC as an additional steric stabilizer to overcome the stability problem observed with Vit. THE TPGS alone. Size analysis revealed a slight increase in size from 0.263 ± 22.12 to 0.296 ± 11μm with a combination that could be due to surface modification of Vit E TPGS-based nanocrystals with HPMC (Table 4). Zeta potential was higher with Vitamin E TPGS (-18.36 ± 0.21) than with combination (-19.1 ± 0.21) and more stability will be the zeta potential. The PDI value observed after one week of combination was also very low whereas a higher value was observed with Vitamin E TPGS alone due to possible recrystallization and polydispersed system formation. As a result, better LNC stabilization was reflected by combination due to improved surface coverage [44]. HPMC present molecule inside the polymeric network to give an amorphous product [45]. HPMC also play a major role in arresting nanocrystal growth possibly due to formation of hydrogen bonding between moisture held and polymer chain of HPMC. It also decreases pore formation from leaching of polymers thus providing good stability [46].

4.6. In-vitro dissolution study

Approximately twice increment was observed with LNC within 1h which continued to increase within 6–8 h for 4 fold of drug dissolution. Probably improved in-vitro dissolution was due to strong hydrophobic interaction between vitamin TPGS and drug molecule [31]. In addition, nanosization increased the exposed surface area for the media to a large extent and thus the rate of dissolution. Additionally, shifting particle size to nano-range increased the solubility of saturation due to increased dissolution pressure as explained by Gao et al., 2008 [47].

4.7. Crystallinity study

PXRD data as shown in Fig. 3A suggested that neither the method of nanoprecipitation nor the stabilizer altered the crystalline nature of the drug. Peaks observed with LZL were wider and diffused where physical mixture showed peak narrowing. LNC had a distinctive pattern with respect to LZL pattern. Horizontal small peak shifts may be due to the presence of a stabilizer protective layer around LZL [21, 35]. The combined results of DSC and PXRD thus confirmed the crystalline nature of prepared nanocrystals although a reduction in crystallinity was observed.

4.8. Ex-Vivo permeation study

Permeation studies reflected similar permeation across different skin layers but significantly different skin retention ($P < 0.05$). Possibly, the dermal delivery was increased as a result of nanocrystals that increased adhesion, solubility, and velocity of dissolution. Enhanced adhesion may be due to increased contact points as a result of nanosizing. Increased solubility of saturation was the result of increased pressure of dissolution which maintained the gradient of concentration between formulation and skin. Increased solubility due to enlarged surface area also resulted in the rapid dissolution of molecules from the surface of nanocrystals resulting in an active deposit in the water phase. Molecules penetrated into the skin were replaced by molecules as depot in the water phase. As a result, increased penetration could result from transfollicular absorption,

reservoir formation, and improved diffusion due to increased concentration gradient between hair follicular space and surrounding cells. Depot formed from a super-saturated solution in hair follicle is due to a limited water/moisture ratio [9].

Higher permeation from formulated gel was observed compared to coarse suspension and nanosuspension (Fig. 4A). Lower cumulative release observed with coarse suspension and nanosuspension could be due to crystallization as a result of methanol evaporation from coarse suspension and nanosuspension. There may be a reduction in concentration gradient and thus in permeation due to crystallization. The higher permeation observed from gel was due to the synergistic results obtained with methanol and propylene glycol which maintained the concentration gradient throughout the application and thus the permeation was slightly higher [25]. In contrast, the lower permeation observed with N-GEL in comparison to D-GEL reflected better drug retention from N-GEL. In addition, drug partition into different skin components was observed where maximum retention with N-Gel was followed by D-gel, Nanosuspension and Coarse Suspension (Fig. 4B). Nanosized systems found to have greater retention with an increase of about 6 percent in drug retention from N-GEL compared to D-GEL, whereas nanosuspension increased by about 8 percent compared to coarse suspension (Fig. 4B). Thus, LNC containing gel could be a promising delivery system for more efficient treatment of dermatophyte infections.

4.9. Antifungal activity

In vitro antifungal activities were encouraging where LNC systems showed significantly different ZOI compared to LZL ($P < 0.05$). Possibly LNC showed wider diffusion and improved efficiency against Candida albicans providing enhanced antifungal action. In addition, the ZOI observed with LNC was also higher than Kansagra H. and Mallick S. 2016 reported for microemulsion-based gel [27]. Thus, formulating LZL as nanocrystals could be an effective way to improve antifungal potency.

5. Conclusion

Luliconazole is a topical antifungal drug with lower bioavailability problem due to its poor aqueous solubility. Improving the solubility could increase the dermal bioavailability and thus LNC were prepared using Vit E TPGS and HPMC as stabilizer. For preparation of luliconazole nanocrystal (LNC), a modified nanoprecipitation method was used involving several optimization parameters such as the stirring speed, solvent system, stabilizer concentration, and temperature. LNC revealed several benefits over parent drug (LZL), including 5-fold enhanced solubility, 4-fold increased dissolution velocity, 6–9% increase in skin retention and a better antifungal activity. Here, LNC loaded topical hydrogel was prepared successfully using carbopol as gelling agent which could potentially be considered as a new antifungal treatment. The results obtained from this study revealed that prepared LNC loaded hydrogel has a great potential to improve the topical delivery of LZL as compared with conventional formulations. In vitro skin permeation and skin retention studies revealed that LNC loaded hydrogel could obviously increases skin permeation of LZL in skin and amount of drug retention in skin layers was significantly enhanced as compared to conventional formulation (coarse suspension). The skin irritation studies in rat was furthermore revealed that irritation potential of LZC hydrogel was minimal. Therefore, it was concluded that LNC loaded hydrogel formulation has a great potential for topical delivery with better drug penetration and retention as well as were safe for treatment of various skin diseases. However, further studies are needed to fully explore these formulations such as extensive pharmacokinetic studies, histopathological studies and toxicity studies. In conclusion, LNC hydrogel could be a new approach which can be applied in future to improve the dermal delivery of drugs with poor aqueous solubility.

Declarations

Author contribution statement

Manish Kumar: Conceived and designed the experiments; Performed the experiments; Analyzed and interpreted the data; Wrote the paper.

Nithya Shanthi: Conceived and designed the experiments; Analyzed and interpreted the data; Wrote the paper.

Shashank Soni: Conceived and designed the experiments; Contributed reagents, materials, analysis tools or data.

Arun Kumar Mahato: Analyzed and interpreted the data; Contributed reagents, materials, analysis tools or data.

P.S. Rajnikanth: Analyzed and interpreted the data; Contributed reagents, materials, analysis tools or data; Wrote the paper.

Funding statement

This research did not receive any specific grant from funding agencies in the public, commercial, or not-for-profit sectors.

Competing interest statement

The authors declare no conflict of interest.

Additional information

No additional information is available for this paper.

Acknowledgements

I would like to thank Virupaksh Organics Ltd., Telangana, India for providing Luliconazole and Antares Health Products Inc., Bhiwandi, India for Vit. E TPGS as the gift sample. My sincere thanks goes to Dr. (Prof.) S. K. Nath, Head of Department of Metallurgical and Materials Engineering (IIT), Roorkee for providing me cooling probe sonicator to conduct size reduction. I also thank Institute Instrumentation Centre (IIC) and Chemistry Department of Indian Institute of Technology (IIT), Roorkee (Uttarakhand) for the evaluation parameters regarding my Research work.

References

[1] Luliconazole, Accession No. DB08933, Available at https://www.drugbank.ca/drugs/DB08933 [Accessed 27 September 2017].

[2] Luliconazole, National Center for Biotechnology Information. PubChem Compound Database; CID=3003141, https://pubchem.ncbi.nlm.nih.gov/compound/3003141 (accessed July 3, 2018). Available at https://pubchem.ncbi.nlm.nih.gov/compound/3003141 [Accessed 27 September 2017].

[3] A. Mundstock, G. Lee, Saturation solubility of nicotine, scopolamine and paracetamol in model stratum corneum lipid matrices, Int. J. Pharm. 473 (1–2) (2014) 232–238.

[4] M. Malamatari, K.M. Taylor, S. Malamataris, D. Douroumis, K. Kachrimanis, Pharmaceutical nanocrystals: production by wet milling and applications, Drug Discov. Today 23 (3) (2018) 534–547.

[5] R.H. Muller, S. Gohla, C.M. Keck, State of the art of nanocrystals-special features, production, nanotoxicology aspects and intracellular delivery, Eur. J. Pharm. Biopharm. 78 (1) (2011) 1–9.

[6] P.P. Ige, R.K. Baria, S.G. Gattani, Fabrication of fenofibrate nanocrystals by probe sonication method for enhancement of dissolution rate and oral bioavailability, Colloids Surfaces B Biointerfaces 108 (2013) 366–373.

[7] T. Hatahet, M. Morille, A. Hommoss, C. Dorandeu, R.H. Muller, S. Begu, Dermal quercetin smartCrystals: formulation development, antioxidant activity and cellular safety, Eur. J. Pharm. Biopharm. 102 (2016) 51–63.

[8] L. Al Shaal, R. Shegokar, R.H. Müller, Production and characterization of antioxidant apigenin nanocrystals as a novel UV skin protective formulation, Int. J. Pharm. 420 (1) (2011) 133–140.

[9] L. Vidlarova, G.B. Romero, J. Hanus, F. Stepanek, R.H. Muller, Nanocrystals for dermal penetration enhancement-Effect of concentration and underlying mechanisms using curcumin as model, Eur. J. Pharm. Biopharm. 104 (2016) 216–225.

[10] T.R. Hoare, D.S. Kohane, Hydrogels in drug delivery: progress and challenges, Polymer 49 (8) (2008) 1993–2007.

[11] F. Laffleur, Evaluation of chemical modified hydrogel formulation for topical suitability, Int. J. Biol. Macromol. 105 (2017) 1310–1314.

[12] W. Liu, M. Hu, W. Liu, C. Xue, H. Xu, X. Yang, Investigation of the carbopol gel of solid lipid nanoparticles for the transdermal iontophoretic delivery of triamcinolone acetonide acetate, Int. J. Pharm. 364 (1) (2008) 135–141.

[13] A. Arellano, S. Santoyo, C. Martın, P. Ygartua, Influence of propylene glycol and isopropyl myristate on the in vitro percutaneous penetration of diclofenac sodium from carbopol gels, Eur. J. Pharm. Sci. 7 (2) (1999) 129–135.

[14] A.S. Zidan, N. Kamal, A. Alayoubi, M. Seggel, S. Ibrahim, Z. Rahman, C.N. Cruz, M. Ashraf, Effect of isopropyl myristate on transdermal permeation of testosterone from carbopol gel, J. Pharm. Sci. 106 (7) (2017) 1805–1813.

[15] N.J. Desai, D.G. Maheshwari, UV spectrophotometric method for the estimation of luliconazole in marketed formulation (lotion), Pharma Sci. Monit. 5 (2) (2014) 48–54.

[16] J. Wang, L. Urban, D. Bojanic, Maximising use of in vitro ADMET tools to predict in vivo bioavailability and safety, Expert Opin. Drug Metabol. Toxicol. 3 (5) (2007) 641–665.

[17] Li Di, Edward H. Kerns, Chapter 23 – Lipophilicity Methods in Drug Like Properties (second ed.) Concepts, Structure Design and Methods from ADME to Toxicity Optimization, Academic press, 2016, pp. 299–306. Available at, https://www.sciencedirect.com/science/article/pii/B978012801076100023X.

[18] U. Bilati, E. Allémann, E. Doelker, Development of a nanoprecipitation method intended for the entrapment of hydrophilic drugs into nanoparticles, Eur. J. Pharm. Sci. 24 (1) (2005) 67–75.

[19] T. Geng, P. Banerjee, Z. Lu, A. Zoghbi, T. Li, B. Wang, Comparative study on stabilizing ability of food protein, non-ionic surfactant and anionic surfactant on BCS type II drug carvedilol loaded nanosuspension: physicochemical and pharmacokinetic investigation, Eur. J. Pharm. Sci. 109 (2017) 200–208.

[20] J.S. Choi, J.S. Park, Effects of paclitaxel nanocrystals surface charge on cell internalization, Eur. J. Pharm. Sci. 93 (2016) 90–96.

[21] B. Mishra, J. Sahoo, P.K. Dixit, Formulation and process optimization of naproxen nanosuspensions stabilized by hydroxy propyl methyl cellulose, Carbohydr. Polym. 127 (2015) 300–308.

[22] D.K. Koradia, H.R. Parikh, Dissolution enhancement of albendazole through nanocrystal formulation, J. Pharm. BioAllied Sci. 4 (Suppl. 1) (2012) S62.

[23] B. Morakul, J. Suksiriworapong, M.T. Chomnawang, P. Langguth, V.B. Junyaprasert, Dissolution enhancement and in vitro performance of clarithromycin nanocrystals produced by precipitation-lyophilization-homogenization method, Eur. J. Pharm. Biopharm. 88 (3) (2014) 886–896.

[24] S. Verma, S. Kumar, R. Gokhale, D.J. Burgess, Physical stability of nanosuspensions: investigation of the role of stabilizers on Ostwald ripening, Int. J. Pharm. 406 (1–2) (2011) 145–152.

[25] X. Zhai, J. Lademann, C.M. Keck, R.H. Muller, Dermal nanocrystals from medium soluble actives–Physical stability and stability affecting parameters, Eur. J. Pharm. Biopharm. 88 (1) (2014) 85–91.

[26] H. Chaudhary, A. Rohilla, P. Rathee, V. Kumar, Optimization and formulation design of carbopol loaded Piroxicam gel using novel penetration enhancers, Int. J. Biol. Macromol. 55 (2013) 246–253.

[27] H. Kansagra, S. Mallick, Microemulsion based antifungal gel of luliconazole for dermatophyte infections: formulation, characterization and efficacy studies, J. Pharmaceut. Investig. 46 (1) (2016) 21–28.

[28] F. Dreher, P. Walde, P.L. Luisi, P. Elsner, Human skin irritation studies of a lecithin microemulsion gel and of lecithin liposomes, Skin Pharmacol. Physiol. 9 (2) (1996) 24–129.

[29] R. Pireddu, C. Caddeo, D. Valenti, F. Marongiu, A. Scano, G. Ennas, F. Lai, A.M. Fadda, C. Sinico, Diclofenac acid nanocrystals as an effective strategy to reduce in vivo skin inflammation by improving dermal drug bioavailability, Colloids Surfaces B Biointerfaces 143 (2016) 64–70.

[30] S.M. Pyo, D. Hespeler, C.M. Keck, R.H. Muller, Dermal miconazole nitrate nanocrystals– formulation development, increased antifungal efficacy & skin penetration, Int. J. Pharm. 531 (1) (2017) 350–359.

[31] I. Ghosh, S. Bose, R. Vippagunta, F. Harmon, Nanosuspension for improving the bioavailability of a poorly soluble drug and screening of stabilizing agents to inhibit crystal growth, Int. J. Pharm. 409 (1–2) (2011) 260–268.

[32] I. Ghosh, D. Schenck, S. Bose, C. Ruegger, Optimization of formulation and process parameters for the production of nanosuspension by wet media milling technique: effect of vitamin E TPGS and nanocrystal particle size on oral absorption, Eur. J. Pharm. Sci. 47 (4) (2012) 718–728.

[33] P.F. Yue, J. Wan, Y. Wang, Y. Li, Y.Q. Ma, M. Yang, P.Y. Hu, H.L. Yuan, C.H. Wang, d-Alpha tocopherol acid polyethylene glycol 1000 succinate, an effective stabilizer during solidification transformation of baicalin nanosuspensions, Int. J. Pharm. 443 (1) (2013) 279–287.

[34] Masuda, T., Pola Pharma Inc. and Nihon Nohyaku Co. Ltd. (2015) Crystal Having crystal Habits and Pharmaceutical Composition Obtained by Processing the crystal. U.S. Patent US20150183766.

[35] R. Kumar, P.F. Siril, Enhancing the solubility of fenofibrate by nanocrystal formation and encapsulation, AAPS PharmSciTech 19 (1) (2017) 284–292.

[36] S. Jana, S. Manna, A.K. Nayak, K.K. Sen, S.K. Basu, Carbopol gel containing chitosan-egg albumin nanoparticles for transdermal aceclofenac delivery, Colloids Surfaces B Biointerfaces 114 (2014) 36–44.

[37] C. Formosa, M. Schiavone, A. Boisrame, M.L. Richard, R.E. Duval, E. Dague, Multiparametric imaging of adhesive nanodomains at the surface of Candida albicans by atomic force microscopy, Nanomed. Nanotechnol. Biol. Med. 11 (1) (2015) 57–65.

[38] N. Sharma, P. Madan, S. Lin, Effect of process and formulation variables on the preparation of parenteral paclitaxel-loaded biodegradable polymeric nanoparticles: a co-surfactant study, Asian J. Pharm. Sci. 11 (3) (2016) 404–416.

[39] S. Kumar, J. Shen, B. Zolnik, N. Sadrieh, D.J. Burgess, Optimization and dissolution performance of spray-dried naproxen nano-crystals, Int. J. Pharm. 486 (1–2) (2015) 159–166.

[40] A. Makhlof, Y. Miyazaki, Y. Tozuka, H. Takeuchi, Cyclodextrins as stabilizers for the preparation of drug nanocrystals by the emulsion solvent diffusion method, Int. J. Pharm. 357 (1) (2008) 280–285.

[41] M. Colombo, S. Staufenbiel, E. Ruhl, R. Bodmeier, In situ determination of the saturation solubility of nanocrystals of poorly soluble drugs for dermal application, Int. J. Pharm. 521 (1) (2017) 156–166.

[42] D. Liu, H. Pan, F. He, X. Wang, J. Li, X. Yang, W. Pan, Effect of particle size on oral absorption of carvedilol nanosuspensions: in vitro and in vivo evaluation, Int. J. Nanomed. 10 (2015) 6425.

[43] Z. Zhou, Q. Li, X.S. Zhao, Evolution of interparticle capillary forces during drying of colloidal crystals, Langmuir 22 (8) (2006) 3692–3697.

[44] I. Ghosh, B. Michniak-Kohn, A comparative study of Vitamin E TPGS/HPMC supersaturated system and other solubilizer/polymer combinations to enhance the permeability of a poorly soluble drug through the skin, Drug Dev. Ind. Pharm. 38 (11) (2012) 1408–1416.

[45] A. Nanda, R.N. Sahoo, A. Pramanik, R. Mohapatra, S.K. Pradhan, A. Thirumurugan, D. Das, S. Mallick, Drug-in-mucoadhesive type film for ocular anti-inflammatory potential of amlodipine: effect of sulphobutyl-ether-beta-cyclodextrin on permeation and molecular docking characterization, Colloids Surfaces B Biointerfaces 1 (172) (2018) 555–564.

[46] B. Panda, A.S. Parihar, S. Mallick, Effect of plasticizer on drug crystallinity of hydroxypropyl methylcellulose matrix film, Int. J. Biol. Macromol. 67 (2014) 295–302.

[47] L. Gao, D. Zhang, M. Chen, Drug nanocrystals for the formulation of poorly soluble drugs and its application as a potential drug delivery system, J. Nanoparticle Res. 10 (5) (2008) 845–862.